


Generalized early dark energy and its cosmological consequences

Tatsuki Kodama,¹ Takumi Shinohara,¹ and Tomo Takahashi²

¹*Graduate School of Science and Engineering, Saga University, Saga 840-8502, Japan*

²*Department of Physics, Saga University, Saga 840-8502, Japan*

 (Received 29 September 2023; accepted 21 February 2024; published 13 March 2024)

We investigate cosmological consequences of a generalized early dark energy (EDE) model where a scalar field behaves as dark energy at various cosmological epochs for a broad range of parameters such as the energy scale and the initial field value. We consider power-law and axion-type potentials for such an EDE field and study how it affects the cosmological evolution. We show that gravitational wave background can be significantly enhanced to be detected in future observations such as LISA and DECIGO in some parameter space. Implications of the EDE model are also discussed for a scenario where a blue-tilted inflationary tensor power spectrum can explain the recent NANOGrav 15-year signal. We argue that the bounds on the reheating temperature can be relaxed compared to the case of the standard thermal history.

DOI: [10.1103/PhysRevD.109.063518](https://doi.org/10.1103/PhysRevD.109.063518)

I. INTRODUCTION

Scalar fields play an important role in various aspects of cosmology. A prime example is the inflation where a scalar field, called inflaton, drives the inflationary expansion and gives the origin of density fluctuations in the Universe.¹ Another one is a quintessence field which can explain dark energy of the Universe.² Scalar fields could also affect the evolution of the Universe not only during inflation and the current accelerating Universe, but also some time in between. Indeed, high-energy theories such as superstring and those with supersymmetry and so on, predict the existence of scalar fields and hence they are expected to be ubiquitous in the early Universe. One of such an example is the moduli field [7–10] which may dominate the Universe at some epoch between the end of inflation and big bang nucleosynthesis, and could affect the cosmological evolution. Yet another example is an early dark energy model [see Refs. [11,12] for a recent review and the references therein, and see, e.g., [13] for possible problems in the early dark energy (EDE) model] where a scalar field gives some contribution to the total energy density at around the radiation-matter equality epoch, which may help to resolve the so-called Hubble tension (see e.g., [14,15] for

the current status of the tension).³ Actually, a scalar field could also help to resolve the Hubble tension in a different manner. For example, there exists a model in which the time variation of the electron mass can be generated by the dynamics of a scalar field, a dilaton [18], and such a time-varying electron mass can significantly reduce the tension [19]. In any case, scalar fields can play an essential role during the evolution of the Universe and have been discussed in various contexts.

A typical behavior of a scalar field is such that it slowly rolls in the early Universe and then starts to oscillate around the minimum of its potential at some point. In many scenarios, the potential of such a scalar field around the minimum is assumed to be a quadratic form (or at least the quadratic term dominates around the minimum), and hence its energy density ρ_χ dilutes as $\rho_\chi \propto a^{-3}$, which is the same scaling as that of matter. However, the potential around the minimum can be different from the quadratic one, and indeed a higher-order polynomial can dominate around its minimum as in the EDE scenario.⁴ In such a case, the energy density of the scalar field dilutes faster than that of matter, i.e., $\rho_\chi \propto a^{-q}$ with $q > 3$ and especially, when $q > 4$, it dilutes faster than radiation, in which the scalar field quickly

¹Even if a scalar field is subdominant during inflation, such a scalar field can generate density fluctuations as in the curvaton scenario [1–3], modulated reheating [4,5] and so on.

²In models with a canonical quintessence, the Hubble constant tends to be even lower than that in the Λ CDM model when fitted to cosmological data such as cosmic microwave background and so on (see, e.g., [6]), and hence it may not be well-motivated from the viewpoint of the H_0 tension.

³Early dark energy may also alleviate another tension, the so-called helium anomaly where a recent measurement of primordial abundance of helium-4 by EMPRESS [16] suggests a nonstandard cosmological scenario, which has been discussed in [17].

⁴Effects of a nonquadratic potential have also been considered in different contexts. One of such examples is the curvaton model where it has been shown that the predictions for primordial non-Gaussianities can be drastically modified from the quadratic potential case [20–29].

disappears and becomes irrelevant for the cosmological evolution after it starts to oscillate. Indeed such a fast-diluting scalar field (a scalar field whose energy density dilutes faster than that of matter and/or radiation) is essential in the EDE model to solve the Hubble tension and has been rigorously investigated [11,12].

In the context of the Hubble tension, the initial amplitude and the parameters in the potential for an EDE field are set such that it starts to oscillate around the epoch of radiation-matter equality and its energy density should give some sizable fractional contribution to the total one, and then quickly dilutes not to affect the cosmic evolution much, which is required to resolve the Hubble tension. However, some level of fine-tuning needs to be done to realize such a situation. From a general ground, a scalar field can dominate the Universe and start to oscillate at some epoch depending on the parameter choice and its initial value. In this spirit, we in this paper consider an EDE field in a general setting to allow various possibilities for its evolution. We refer to such an EDE field as “generalized early dark energy” and investigate its cosmological consequences.⁵ To this end, first we identify what energy scale for the potential and the initial value for the scalar field affect which epoch in the course of the history of the Universe. Indeed, in a broad range of the parameter space, such a scalar field can dominate the Universe during its slow-rolling phase, which gives rise to a short period of inflation. After it starts to oscillate, we assume that its energy density dilutes quickly such that it becomes irrelevant to the cosmological evolution as in usual EDE models as a solution to the Hubble tension. Interestingly, in such a case, gravitational wave (GW) spectrum can be enhanced and could be detected in the future experiments. We identify the parameter space where such an enhancement occurs. We also discuss the implications of the generalized EDE for the recent result of NANOGrav 15 year data on GW background [31,32], particularly in models where the inflationary blue-tilted tensor power spectrum can explain the NANOGrav signal.

The organization of this paper is as follows. In the next section, we describe the setup of our scenario of a generalized early dark energy field and define several quantities that facilitate our discussion. Its cosmological evolution will also be discussed in some detailed manner. Then in Sec. III, we investigate GW spectrum in such a model, and investigate its detectability in some future experiments such as LISA and DECIGO. Implications for the NANOGrav is also discussed. In the final section, conclusions and a discussion are given.

⁵Another possible extension of an EDE model is to assume a general equation of state for the initial and final EDE fluid, which has been investigated in [30].

II. EVOLUTION OF GENERALIZED EARLY DARK ENERGY

In this section, first we describe the setup of our scenario and summarize the formalism to investigate cosmological consequences of a generalized EDE. Then we discuss the evolution of the EDE field and its effects on the cosmic expansion. We also investigate possible initial values and the energy scale of the EDE field from the stochastic formalism argument.

A. Setup

We follow the cosmic evolution from the time just after the end of inflation to the present epoch and assume that there exist a scalar field χ (a generalized EDE field), radiation and matter components in the Universe.⁶ The equation of motion for χ and the Friedmann equation is given by

$$\ddot{\chi} + 3H\dot{\chi} + V_{,\chi}(\chi) = 0, \quad (2.1)$$

$$H^2 = \frac{\rho_{\text{tot}}}{3M_{\text{Pl}}^2} = \frac{1}{3M_{\text{Pl}}^2} (\rho_r + \rho_m + \rho_{\text{DE}} + \rho_\chi), \quad (2.2)$$

where $V(\chi)$ represents a potential of the scalar field. A dot denotes a derivative with respect to the cosmic time t and $V_{,\chi}(\chi) = dV(\chi)/d\chi$, $a(t)$ is the scale factor of the Universe, normalized to be unity at present, $H \equiv \dot{a}/a$ is the Hubble parameter, $M_{\text{Pl}} \equiv 1/\sqrt{8\pi G} \simeq 2.436 \times 10^{18}$ GeV is the reduced Planck mass. ρ_{tot} is the total energy density and ρ_r , ρ_m , and ρ_{DE} are those of radiation, matter and dark energy components, respectively. ρ_χ is the energy density of χ which is given as

$$\rho_\chi = \frac{\dot{\chi}^2}{2} + V(\chi). \quad (2.3)$$

In this work, we consider the following two potentials for the EDE field χ :

$$V(\chi) = V_0 \left(\frac{\chi}{M_{\text{Pl}}} \right)^p \quad (\text{power-law}), \quad (2.4)$$

$$V(\chi) = V_0 \left(1 + \cos \frac{\chi}{f_a} \right)^n \quad (\text{axion-type}), \quad (2.5)$$

where p and n represent the power-law index, V_0 is the energy scale of the potential, and f_a is the decay constant.

⁶Although we include a cosmological constant as the late-time dark energy component to evaluate the evolution of the scale factor up to the present epoch for completeness, it is irrelevant to our arguments below. In our calculation, the cosmological parameters are set to the ones given by Planck observation 2018 [33]: $h = 0.6766$ and $\Omega_m h^2 = 0.1424$ when necessary.

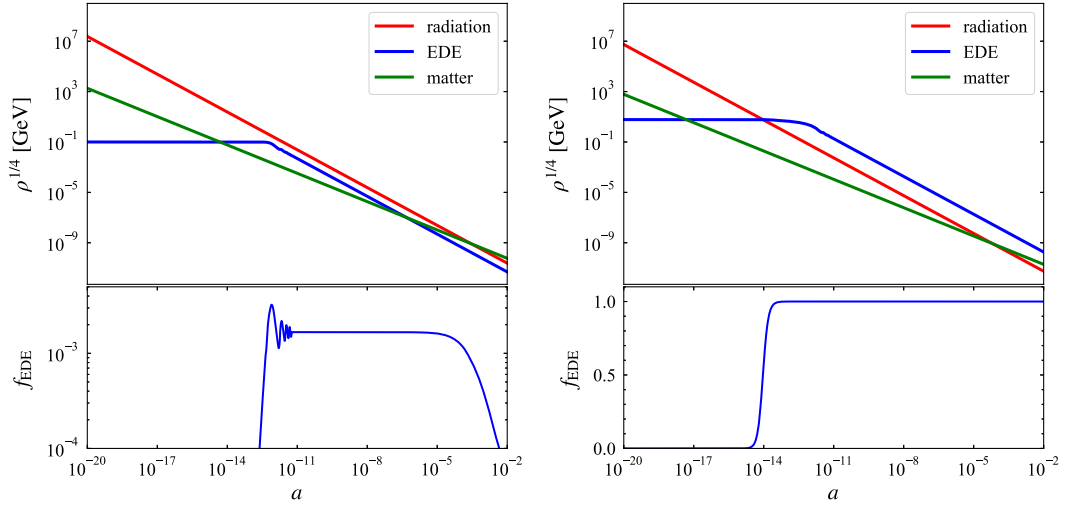


FIG. 1. Evolution of energy densities of EDE, radiation and matter. In this figure, we assume the power-law potential with $p = 4$ and take $\chi_{\text{ini}} = 0.1M_{\text{Pl}}$ and $V_0^{1/4} = 1 \text{ GeV}$ (left panel), and $\chi_{\text{ini}} = 6M_{\text{Pl}}$ and $V_0^{1/4} = 1 \text{ GeV}$ (right panel).

These types of potential, particularly with $p \geq 4$ and $n \geq 2$ are well investigated in the context of the Hubble tension [12] since such values of p and n allow the energy density of EDE dilutes faster than matter and quickly becomes irrelevant to the cosmic evolution, particularly when the Universe becomes matter dominated. Moreover, the parameters in the potential need to be tuned to affect the evolution around radiation-matter equality when one tries to resolve the Hubble tension. Below we investigate what parameter values influence the evolution of the Universe, when and to what extent. To this end, we follow the evolution of the EDE field from the time just after the reheating has been completed, which is regarded as the initial time in our calculation. We note that, although we specify the energy

scale of inflation, we do not need to assume an explicit form for the inflaton potential in the following argument.

In Figs. 1 and 2, we show some examples of the thermal history in the generalized EDE model with the power-law potential. Since the energy density of an oscillating scalar field under the potential of $V(\chi) \propto \chi^p$ with $p > 0$ scales as [34]

$$\rho_\chi \propto a^{-6p/(p+2)}. \quad (2.6)$$

Notice that ρ_χ for $p = 4$ scales as the same as that of radiation, and when $p > 4$, it dilutes faster than radiation. In the following argument, we also use the effective

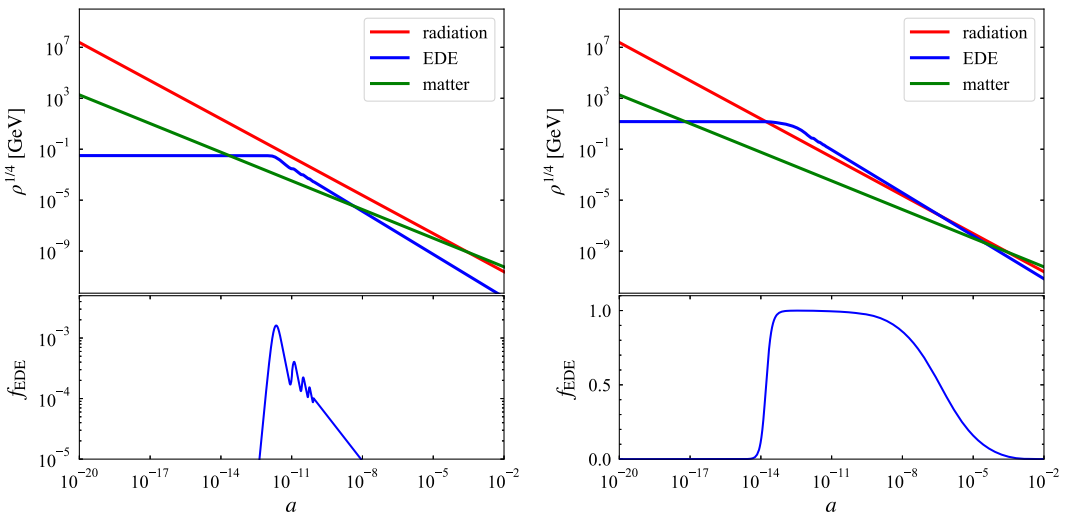


FIG. 2. The same as Fig. 1, but for the power-law potential with $p = 6$. Here we take $\chi_{\text{ini}} = 0.1M_{\text{Pl}}$ and $V_0^{1/4} = 1 \text{ GeV}$ (left panel) and $\chi_{\text{ini}} = 6M_{\text{Pl}}$ and $V_0^{1/4} = 1 \text{ GeV}$ (right panel).

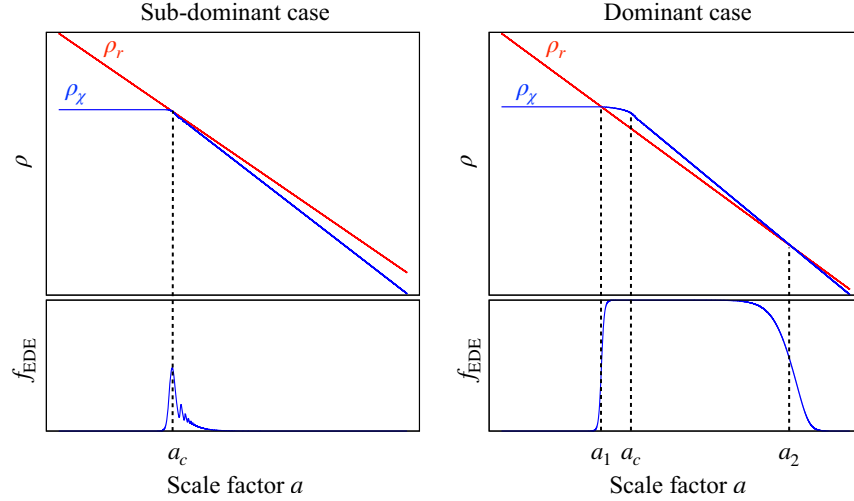


FIG. 3. Schematic figure describing the characteristic scale factor a_1 , a_c , and a_2 for the case of $p > 4$. The right (left) panel corresponds to the case where the EDE field dominates at some epoch (always subdominant) during the course of the history of the Universe. Red and blue lines describe energy densities of radiation and the EDE, respectively. The bottom panel shows the evolution of f_{EDE} . The scale factor a_c is defined as the one at which the f_{EDE} takes the maximum value. a_1 and a_2 correspond to the epoch at which the EDE energy density supersedes and is overtaken by that of radiation, respectively. Notice that a_1 and a_2 only appear when the EDE field dominates the Universe at some time (right panel).

equation of state w for the oscillating EDE field which is related to p as

$$w = \frac{p-2}{p+2}. \quad (2.7)$$

Here we only show the cases with the power-law potential since the axion-type potential (2.5) around the minimum has a form $V(\chi) \propto \chi^{2n}$, and then the evolution of the axion-type EDE is quite similar to the one for the power-law type with $n = p/2$. In Fig. 1, the case for the power-law potential with $p = 4$ is shown for $(\chi_{\text{ini}}, V_0^{1/4}) = (0.1M_{\text{Pl}}, 1 \text{ GeV})$ (left panel) and $(6M_{\text{Pl}}, 1 \text{ GeV})$ (right panel). The case for the power-law potential with $p = 6$ is also shown in Fig. 2, in which the values of χ_{ini} and V_0 are taken to be the same as those in Fig. 1. In the left panel (in both Figs. 1 and 2), we take the parameters such that the EDE field does not dominate the Universe during the whole history, on the other hand, the right panel corresponds to the case where the EDE field dominates the Universe during its slow-rolling phase and quasi-de Sitter phase appears before the EDE field starts to oscillate. Since ρ_χ for the case of $p = 4$ decreases as the same as that of radiation, the Universe is dominated by EDE until matter does. It should be noted that a cosmological scenario where the oscillating EDE field dominates the Universe until matter supersedes it would be excluded by cosmic microwave background (CMB) observations, the case shown in the right panel of Fig. 1 is just for illustration purposes.

In the bottom panels of the figures, we also depict the evolution of f_{EDE} which represents the fraction of ρ_χ in the total energy density, defined as

$$f_{\text{EDE}} \equiv \frac{\rho_\chi}{\rho_{\text{tot}}} = \frac{\rho_\chi}{\rho_\chi + \rho_r + \rho_m + \rho_{\text{DE}}}. \quad (2.8)$$

We also define the parameter a_c and χ_c which denote the scale factor and the value of χ field at which f_{EDE} takes its maximum value.⁷ In Fig. 3, the schematic picture is shown to explain which epoch corresponds to a_c .

When the EDE dominates the Universe and quasi-de Sitter phase appears at some epoch as in the right panel of Figs. 1 and 2, we define yet another scale factor (or time), denoted as a_1 , at which the energy density of EDE supersedes that for radiation (see the right panel of Fig. 3). The scale factor a_1 can be evaluated as

$$\frac{a_1}{a_R} \simeq \left(\frac{\rho_r(T_R)}{V(\chi_{\text{ini}})} \right)^{1/4}, \quad (2.9)$$

where χ_{ini} is the initial value of χ field, a_R and T_R are the scale factor and the temperature at the time of reheating, and $\rho_r(T_R)$ is radiation energy density at the reheating after inflation which is given by

$$\rho_r(T_R) = \frac{\pi^2}{30} g_*(T_R) T_R^4, \quad (2.10)$$

with $g_*(T_R)$ the degrees of freedom at the time of reheating. In our numerical calculation, we assume that the inflationary

⁷This epoch roughly corresponds to the time when the EDE field starts to oscillate and $H \sim m_{\text{eff}} \equiv \sqrt{V''}$ holds. However, this rough estimate fails especially when the quasi-de Sitter phase appears. Therefore we evaluate a_c from the numerical calculation with the definition described here.

Hubble scale is $H_{\text{inf}} = 10^{13}$ GeV and the reheating temperature is $T_R = 10^{15}$ GeV for definiteness unless otherwise stated although their actual numbers do not affect our arguments. The above choice of H_{inf} and T_R almost corresponds to the case of the instantaneous reheating. For $p > 4$, the energy density of an oscillating EDE field dilutes faster than radiation, and hence after the EDE field starts to oscillate, there appears the second equality when ρ_χ is overtaken by ρ_r , which we denote by a_2 (see the right panel of Fig. 3). We can express a_2 by using a_c and the effective equation of state parameter w for an oscillating EDE field as

$$\frac{a_2}{a_c} \simeq \left[\left(\frac{a_c}{a_R} \right)^4 \frac{V(\chi_c)}{\rho_r(T_R)} \right]^{1/(3w-1)}. \quad (2.11)$$

The analytic expression for a_c is given in the next section.

B. Estimates for $f_{\text{EDE}}(a_c)$ and a_c

In the context of the Hubble tension, f_{EDE} is an important parameter since the fraction of energy density of EDE determines its effects on the CMB power spectrum. Actually, as many analysis indicates, the EDE should give some fractional contribution to the total energy density of the Universe as $f_{\text{EDE}} = \mathcal{O}(0.01) - (0.1)$ at around the radiation-matter equality, i.e., $a_c \sim a_{\text{eq}}$, to resolve the Hubble tension [12]. We note that EDE not only affects the background dynamics, but also the evolution of the perturbation, which helps to reduce the tension. The fraction of EDE f_{EDE} suitable to resolve the Hubble tension has been obtained including effects of the perturbations, then $f_{\text{EDE}} = \mathcal{O}(0.01) - (0.1)$ is preferred (see Ref. [12] and the references therein).

Here we investigate what values of $f_{\text{EDE},c} (\equiv f_{\text{EDE}}(a_c))$ and a_c are obtained in a broad range of the parameter space. In Fig. 4, we show contours of $f_{\text{EDE},c}$ and a_c in the plane of

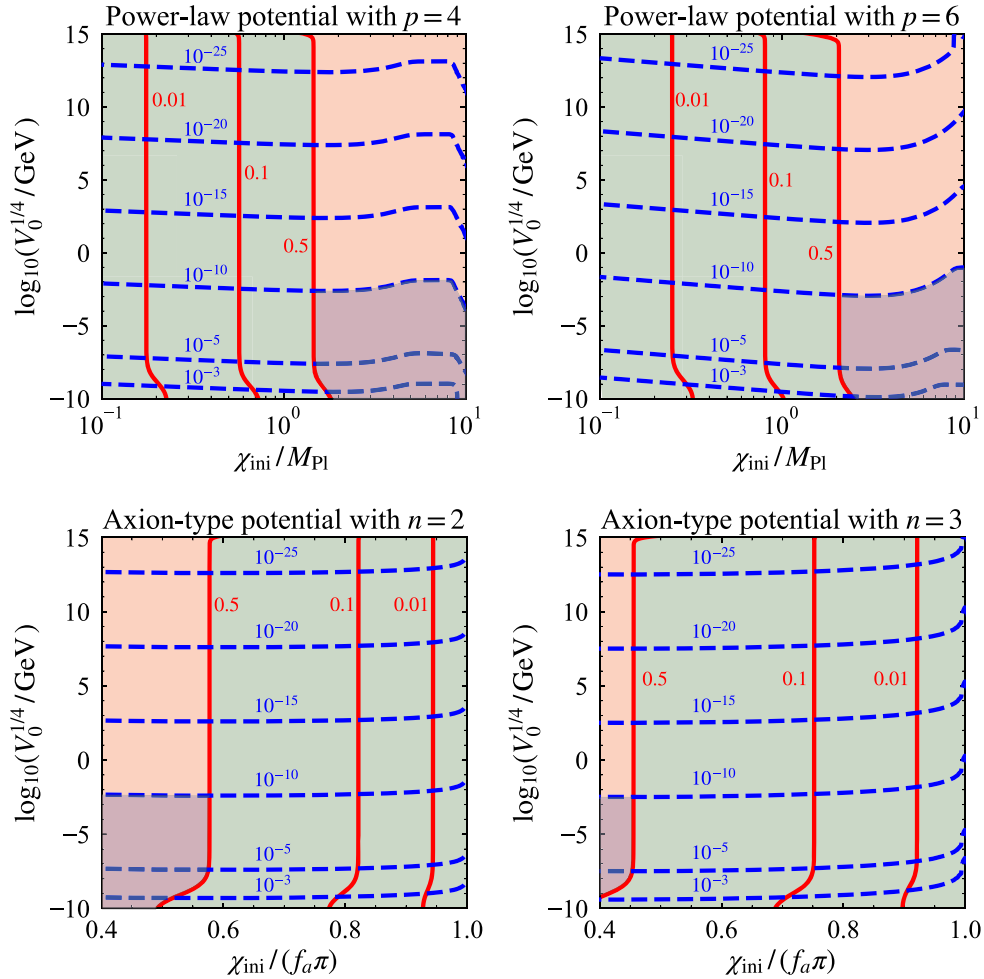


FIG. 4. Contour plots of $f_{\text{EDE},c}$ (red) and a_c (blue) in the $\chi_{\text{ini}}-V_0$ plane. The upper and bottom panels show the power-law and the axion-type potentials with $p = 2n = 4$ (left panels) and $p = 2n = 6$ (right panels), respectively. The red and green region correspond to the case with $f_{\text{EDE},c} > 0.5$ and $f_{\text{EDE},c} < 0.5$, respectively. In the blue region, the EDE dominates after the BBN epoch, which would contradict cosmological observations.

χ_{ini} , and V_0 for the cases with the power-law (top panels) and the axion-type (bottom panels) potentials. When the EDE field dominates the Universe to generate the quasi-de Sitter phase after the epoch of big bang nucleosynthesis (BBN), the subsequent thermal history of the Universe is significantly changed, which would contradict cosmological observations. On the other hand, when such de Sitter phase appears before the BBN epoch, various cosmological constraints would be irrelevant and it can give an interesting implication for the GW observations which will be discussed in the next section. From the figure, one can also easily see what values of χ_{ini} and V_0 can realize $f_{\text{EDE},c} = \mathcal{O}(0.01) - (0.1)$ and $a_c = \mathcal{O}(10^{-4})$, which are necessary to resolve the Hubble tension, where the initial field value is sub-Planckian for the power-law potential case. On the other hand, for the case of the axion-type potential, the decay constant f_a and the initial value of the EDE field tend to be near Planckian to resolve the Hubble tension, which may raise an issue from the perspective of the weak gravity conjecture [35,36]. In the parameter space where EDE dominates to give a quasi-de Sitter phase (e.g., $f_{\text{EDE}} > 0.5$), the GW spectrum can be enhanced as we will discuss in the next section, however the initial field value becomes super-Planckian in the power-law potential case. In such a region, quantum gravity effects should be considered, which is phrased by the so-called super-Planckian problem [37,38] and the trans-Planckian censorship conjecture [39], although such a super-Planckian field excursion does not necessarily lead to the problem since it does not always mean the Planckian energy density.

We can analytically understand the behavior of $f_{\text{EDE},c}$ and a_c in the $\chi_{\text{ini}}-V_0$ plane as follows. First of all, $V(\chi_c)$ and $f_{\text{EDE},c}$ at $a = a_c$ are related as

$$V(\chi_c) \simeq \frac{f_{\text{EDE},c}}{1 - f_{\text{EDE},c}} \rho_r(a_c), \quad (2.12)$$

where we consider the case where the Universe is radiation dominated at $a = a_c$, and we approximate the EDE energy density as $\rho_\chi(a_c) \simeq V(\chi_c)$. For the power-law potential (2.4), by taking the logarithm of both sides of Eq. (2.12), one obtains

$$\log_{10} \left(\frac{V_0^{1/4}}{M_{\text{Pl}}} \right) + \frac{p}{4} \log_{10} \frac{\chi_c}{M_{\text{Pl}}} = \frac{1}{4} \log_{10} \frac{f_{\text{EDE},c}}{1 - f_{\text{EDE},c}} + \log_{10} \left(\frac{\rho_r(a_c)^{1/4}}{M_{\text{Pl}}} \right). \quad (2.13)$$

Actually $\rho_r(a_c)$ can be written with χ_{ini} and V_0 . Until the time when $a \simeq a_c$, the slow-roll approximation can be adopted for the equation of motion for the EDE field. By integrating Eq. (2.1) from a_R to a_c under this approximation, one obtains

$$- \int_{\chi_{\text{ini}}}^{\chi_c} \frac{d\chi}{V'} \simeq M_{\text{Pl}}^2 \int_{a_R}^{a_c} \frac{d \ln a}{\rho_{\text{tot}}(a)}. \quad (2.14)$$

where the left-hand side of the above equation can be integrated as

$$- \int_{\chi_{\text{ini}}}^{\chi_c} \frac{d\chi}{V'(\chi)} \simeq \frac{1}{p(p-2)} \frac{M_{\text{Pl}}^2}{V_0} \left[\left(\frac{\chi_c}{M_{\text{Pl}}} \right)^{-(p-2)} - \left(\frac{\chi_{\text{ini}}}{M_{\text{Pl}}} \right)^{-(p-2)} \right]. \quad (2.15)$$

The evaluation of the right-hand side of (2.14) depends on whether the EDE dominates the Universe at $a = a_c$ or not, we discuss each case separately below.

1. Case with EDE subdominant at a_c

We first consider the case where the EDE is subdominant at $a = a_c$. In this case, the Universe is radiation dominated between a_R and a_c , and hence, by replacing ρ_{tot} with ρ_r in the right-hand side of (2.14), we obtain

$$\frac{1}{p(p-2)} \frac{M_{\text{Pl}}^2}{V_0} \left[\left(\frac{\chi_c}{M_{\text{Pl}}} \right)^{-(p-2)} - \left(\frac{\chi_{\text{ini}}}{M_{\text{Pl}}} \right)^{-(p-2)} \right] \simeq \frac{M_{\text{Pl}}^2}{4\rho_r(a_c)}, \quad (2.16)$$

where we have used the approximation that $\rho_r(a_R) \gg \rho_r(a_c)$. Putting the above expression into Eq. (2.13), we have

$$\frac{f_{\text{EDE},c}}{1 - f_{\text{EDE},c}} = \frac{4}{p(p-2)} C^2 (1 - C^{p-2}) \left(\frac{\chi_{\text{ini}}}{M_{\text{Pl}}} \right)^2, \quad (2.17)$$

where we used $\chi_c = C\chi_{\text{ini}}$ with C being constant which holds for $\chi_{\text{ini}} \leq \mathcal{O}(1)$, and our numerical analysis indicates that $C \simeq 0.65$. From Eq. (2.17), we can see that f_{EDE} does not depend on V_0 when the EDE is subdominant at $a = a_c$, i.e., $f_{\text{EDE},c} < 0.5$ and $a_c < a_{\text{eq}}$. From Eq. (2.16), we can express a_c by using V_0 and χ_{ini} as

$$\frac{a_c}{a_R} \simeq \left[\frac{p(p-2)}{4} \frac{V_0}{\rho_r(T_R)} \left(\frac{\chi_{\text{ini}}}{M_{\text{Pl}}} \right)^{p-2} \right]^{-1/4}. \quad (2.18)$$

We can also consider the case where f_{EDE} takes its maximum value during the matter-dominated epoch, namely $a_{\text{eq}} < a_c$. In this case, by replacing $\rho_r(a_c)$ by $\rho_m(a_c)$ in Eq. (2.12) and $\rho_{\text{tot}}(a)$ by $\rho_r(a) + \rho_m(a)$ in Eq. (2.14), and then integrating from a_R to a_c , we can find that the $f_{\text{EDE},c}$ depends on both V_0 and χ_{ini} , contrary to Eq. (2.17) where $a = a_c$ occurs during radiation-dominated epoch. The dependence on V_0 and χ_{ini} can be found in Fig. 4.

2. Case with EDE dominant at a_c

In this case, we can integrate the right-hand side of (2.14), for $a_c \ll a_{\text{eq}}$, as

$$\begin{aligned} M_{\text{Pl}}^2 \int_{a_r}^{a_c} \frac{d \ln a}{\rho_r(a) + \rho_\chi} &\simeq M_{\text{Pl}}^2 \left[\int_{a_r}^{a_1} \frac{d \ln a}{\rho_r(a)} + \int_{a_1}^{a_c} \frac{d \ln a}{\rho_\chi} \right] \\ &\simeq M_{\text{Pl}}^2 \left[\frac{1}{4\rho_r(a_1)} + \frac{1}{V(\chi_c)} \ln \frac{a_c}{a_1} \right]. \end{aligned}$$

Thus, the scale factor a_c is roughly estimated by

$$\frac{a_c}{a_1} \simeq \exp \left[\frac{p^{p-1}}{2^{p/2}(p-2)} \left(\frac{\chi_{\text{ini}}}{M_{\text{Pl}}} \right)^{-p} \left\{ \left(\frac{\chi_{\text{ini}}}{M_{\text{Pl}}} \right)^2 - \frac{p(p-2)}{4} \right\} \right], \quad (2.19)$$

where we have expressed χ_c with χ_{ini} by using the same procedure as done for the standard inflation case (see, e.g., [40]). The above expression can be inserted to Eq. (2.11) to obtain a_2 .

From the above argument, one can see that $f_{\text{EDE},c}$ only depends on χ_{ini} when $a_c < a_{\text{eq}}$, which explains the behavior of the contours of $f_{\text{EDE},c}$ in most region of Fig. 4. Although we have considered the power-law potential case in the above argument, the same also applies to the axion-type potential (2.5), which explains the behavior of $f_{\text{EDE},c}$ in the bottom panels of Fig. 4.

C. Estimate of χ_{ini} from stochastic argument

The EDE field χ considered in this paper can be regarded as a spectator field whose contribution to the energy density is negligible during the inflationary era. When a spectator field is light enough, the quantum diffusion drives the distribution of its field value to reach an equilibrium one, which can be discussed based on the stochastic formalism [41–44] and a typical value of χ_{ini} can be inferred given the inflationary energy scale H_{inf} and the parameter in the potential of χ . Here we briefly discuss such a typical value of χ_{ini} .

The field value of χ follows the Langevin equation:

$$\frac{d\chi(N)}{dN} = -\frac{V_{,\chi}(\chi)}{3H^2} + \frac{H}{2\pi} \xi(N), \quad (2.20)$$

where we take the number of e -folds $N \equiv \ln a$ as a time variable and $\xi(N)$ is a Gaussian white noise. The first and second terms on the right-hand side correspond to classical motion and quantum fluctuations, respectively.

From the above equation, we can get the Fokker-Planck equation as [42]

$$\frac{\partial P(N, \chi)}{\partial N} = \frac{\partial}{\partial \chi} \left[\frac{\partial V(\chi)}{\partial \chi} \frac{P(N, \chi)}{3H^2} + \frac{H^2}{8\pi^2} \frac{\partial P(N, \chi)}{\partial \chi} \right], \quad (2.21)$$

where $P(N, \chi)$ is the probability distribution function (PDF) of the field value of a spectator field χ . An equilibrium solution for $P(N, \chi)$ can be found as [43,44]

$$P_{\text{stat}}(\chi) \propto \exp \left[-\frac{8\pi^2 V(\chi)}{3H_{\text{inf}}^4} \right]. \quad (2.22)$$

Here, we assume that the PDF relaxes to an equilibrium stationary solution by the end of inflation. We can obtain a typical value of the spectator field by setting the absolute value of the exponent approximately equal to unity.

Based on the argument above, we can estimate the values of χ_{ini} and V_0 , which are depicted in Fig. 5 for a given H_{inf} . From the figure, one can see that when the inflationary Hubble scale is $H_{\text{inf}} = 10^{13}$ GeV (10^6 GeV), the scale factor at which the EDE takes its maximum contribution to the total energy density is $a_c = \mathcal{O}(10^{-26}) - \mathcal{O}(10^{-25})[\mathcal{O}(10^{-19}) - \mathcal{O}(10^{-18})]$ for the power-law potential, which is much earlier than the CMB and even BBN epoch. As already mentioned, to resolve the Hubble tension in the framework of the EDE model, one needs to have $a_c = \mathcal{O}(10^{-4})$. Figure 4 indicates that this can be realized when $V_0^{1/4} \simeq 10^{-9}$ GeV, which corresponds to a relatively

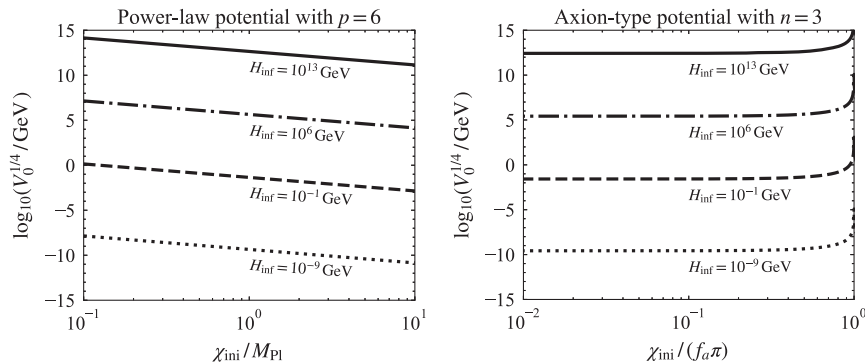


FIG. 5. Contours of H_{inf} suggested from the stochastic argument in the $\chi_{\text{ini}}-V_0$ plane for the power-law (left) and the axion-type (right) potentials with $p = 2n = 6$.

low inflationary scale of $H_{\text{inf}} = \mathcal{O}(10^{-9})$ GeV as seen from Fig. 5.

From the discussion here, one can notice that a low-scale inflation is suggested to resolve the Hubble tension, based on the stochastic argument when the equilibrium distribution is reached during inflation.⁸ For the axion-type potential, we can also draw almost the same conclusion.

III. GRAVITATIONAL WAVES SPECTRUM

In this section, we discuss the consequences of the generalized EDE to the GW spectrum, particularly for the case where the EDE dominates the Universe at some point and, then subsequently its energy density dilutes faster than radiation, i.e., $n > 4$ and $p > 2$ for the power-law and axion-type potentials, respectively.⁹

A. Gravitational waves spectrum

First we briefly describe how the GW spectrum is calculated following the standard procedure. The equation of motion for tensor perturbation in the transverse-traceless gauge in the Fourier space $h_{\mathbf{k}}^{\lambda}$ for the polarization $\lambda = (+, \times)$ is written by

$$\ddot{h}_{\mathbf{k}}^{\lambda} + 3H\dot{h}_{\mathbf{k}}^{\lambda} + \frac{k^2}{a^2}h_{\mathbf{k}}^{\lambda} = 0. \quad (3.1)$$

The GW spectrum, which is the energy density of GWs normalized by the critical energy density per logarithmic interval, is given by

$$\Omega_{\text{GW}}(k) = \frac{1}{12} \left(\frac{k}{aH} \right) \mathcal{P}_T(k) T_T^2(k). \quad (3.2)$$

Here $T_T(k)$ is the transfer function and $\mathcal{P}_T(k)$ is the primordial tensor power spectrum, which is assumed to have the power-law form expressed by

$$\mathcal{P}_T(k) = A_T \left(\frac{k}{k_*} \right)^{n_T}, \quad (3.3)$$

where A_T is the amplitude of the primordial GWs at the pivot scale k_* and n_T is the tensor spectral index. Here we choose the pivot scale as $k_* = 0.05 \text{ Mpc}^{-1}$. The amplitude of the tensor power spectrum can be determined by the inflationary energy scale, namely $\mathcal{P}_T = (8/M_{\text{Pl}}^2)(H_{\text{inf}}/2\pi)^2$. To describe the size of primordial GW spectrum, we usually use the tensor-to-scalar ratio which is defined by

⁸Whether the equilibrium distribution is realized or not depends on the potential of the inflaton [44].

⁹Actually resonant amplification of EDE field fluctuations can give sizable GW background in these kind of potentials [45]. The frequency range is somewhat different from the one discussed here, but such GW background could be another signature of the generalized EDE.

TABLE I. The effective equation of state parameter for an oscillating scalar field w , the indices β and γ for the scaling of the oscillating EDE energy density $\rho_{\text{EDE}} \propto a^{\beta}$ and the GW spectrum $\Omega_{\text{GW}} \propto k^{\gamma}$, respectively, for p (power-law potential) or n (axion-type potential).

$n, p/2$	1	2	3	4	...	∞
w	0	1/3	1/2	3/5	...	1
β	-3	-4	-9/2	-24/5	...	-6
γ	-2	0	2/5	4/7	...	1

$$r = \frac{A_T}{A_S}, \quad (3.4)$$

where A_S is the amplitude of the scalar primordial spectrum at the pivot scale k_* . In the following calculation, we take $r = 10^{-3}$ which is well inside the 2σ bound given by the Planck observation 2018 [33] and the BICEP/Keck Collaboration 2018 [46] for illustration. Since the amplitude of the scalar power spectrum is given as $A_S = 2.1 \times 10^{-9}$ [33], the above value of r gives the energy scale of inflation as $H_{\text{inf}} \approx 10^{13} \text{ GeV}$.¹⁰ Once r is given, for the single-field inflation models, the tensor spectral index n_T can be determined from the so-called consistency relation $n_T = -r/8$.

We numerically solve the equation of motion for $h_{\mathbf{k}}^{\lambda}$ to obtain the transfer function in models with the generalized EDE. The transfer function depends on the background equation of state [47–50], and the behavior of the GW spectrum can be easily captured by noticing that Ω_{GW} scales as

$$\Omega_{\text{GW}} \propto k^{2(3w-1)/(3w+1)} \propto f^{2(3w-1)/(3w+1)}, \quad (3.5)$$

where w is the equation of state parameter of the dominant component during the time when the mode k enters the horizon and f is the frequency corresponding to the mode k . Since the effective equation of state parameter for an oscillating scalar field is given by $w = (p-2)/(p+2)$ for a power-law potential $V(\chi) \propto \chi^p$, the GW spectrum is enhanced during when the oscillating EDE dominates the Universe when $p > 4$ ($n > 2$ for the axion-type potential).¹¹ We summarized the scaling of the energy density of the oscillating EDE and the GW spectrum in Table I.

¹⁰Using the definition of \mathcal{P}_T , (3.4), and the Planck normalization $A_S = 2.1 \times 10^{-9}$, we can estimate the energy scale during inflation as

$$H_{\text{inf}} = 7.84 \times 10^{12} \sqrt{\frac{r}{10^{-3}}} \text{ GeV}.$$

¹¹Actually, when $f_{\text{EDE,c}} \sim 0.5$, the motion of an EDE field can induce an oscillation in the Hubble parameter, which can make some peaks/dips in the GW spectrum [51]. However, in the case of $f_{\text{EDE,c}} > 0.5$, the enhancement discussed here hides such an effect.

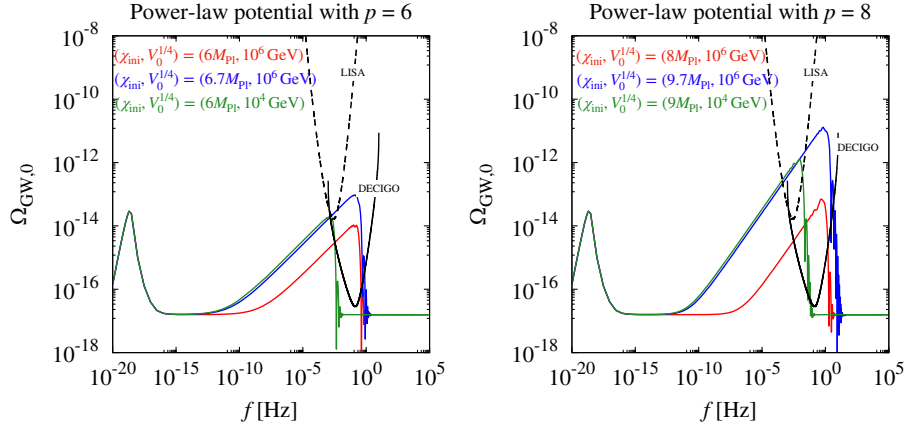


FIG. 6. The GW spectrum for the case of the power-law potential with several values of V_0 and χ_{ini} for the cases with $p = 6$ (left) and 8 (right). In the left panel, we take the parameters as $(\chi_{\text{ini}}, V_0^{1/4}) = (6M_{\text{Pl}}, 10^6 \text{ GeV})$ (red), $(6.7M_{\text{Pl}}, 10^6 \text{ GeV})$ (blue), and $(6M_{\text{Pl}}, 10^4 \text{ GeV})$ (dashed green). In the right panel, $(\chi_{\text{ini}}, V_0^{1/4}) = (8M_{\text{Pl}}, 10^6 \text{ GeV})$ (red), $(9.7M_{\text{Pl}}, 10^6 \text{ GeV})$ (blue), and $(9M_{\text{Pl}}, 10^4 \text{ GeV})$ (dashed green). The black solid and dashed lines represent the PLISCs for DECIGO and LISA, respectively.

In Fig. 6, we show the GW spectra for the power-law potential with several values of χ_{ini} and V_0 . We show the case with $p = 6$ (left) and $p = 8$ (right). For comparison, we also depict the power-law integrated sensitivity curves (PLISCs) [52] for future interferometer observations such as LISA [53] and DECIGO [54]. As seen from the figure, some range of the parameters can predict the GW signal detectable at LISA and DECIGO. Since the effective equation of state parameter w for an oscillating EDE field is $w = 1/2$ for $p = 6$ and $w = 3/5$ for $p = 8$, which indicates that the GW spectrum for the frequency mode which reenter the horizon during the oscillating EDE-dominated phase scales as $\Omega_{\text{GW}} \propto k^{2/5}$ and $\Omega_{\text{GW}} \propto k^{4/7}$ for $p = 6$ and 8 , respectively as shown in Table I. A larger p gives a steeper slope for the increase of the GW spectrum, and hence the case of a larger p allows more parameter space for the detection of GWs. In particular, the case with $p = 2n = \infty$ gives $\Omega_{\text{GW}} \propto k$, which is the same as that for the kination one. GWs in models with kination have been studied in various context, for recent works, see e.g., [55,56].

Here we only show the GW spectrum for the power-law potential case, however, the case of the axion-type potential gives almost the same spectrum as that for the power-law one by identifying $n = p/2$. Therefore we do not show the axion-type potential case here.

B. Detectable region in LISA and DECIGO

In this section, we investigate what values of χ_{ini} and V_0 can predict the stochastic GWs detectable in future observations such as LISA and DECIGO. To quantify the detectability over a wide range of the parameter space, we introduce the signal-to-noise ratio (SNR) written by

$$q = \sqrt{t_{\text{obs}} \int_{f_{\text{min}}}^{f_{\text{max}}} df \left(\frac{\Omega_{\text{GW}}(f)}{\Omega_{\text{noise}}(f)} \right)^2}, \quad (3.6)$$

where t_{obs} is observing time and we set it as $t_{\text{obs}} = 1 \text{ yr}$, f_{max} and f_{min} represent the upper and lower bounds of the frequency range corresponding observations [52,57]. Here the noise spectrum is denoted by Ω_{noise} . If the SNR exceeds a threshold $\rho_{\text{thr}} = 1$ for a parameter set (χ_{ini}, V_0) , we regard that future observations would detect the GWs enhanced by the generalized EDE model.

As shown in Fig. 6, with some parameter choice, the GW spectrum in the generalized EDE model can be well above the PLISCs for LISA and DECIGO. The PLISCs corresponds to the spectrum giving $q_{\text{thr}} = 1$, which means that the SNR is evaluated as $q < q_{\text{thr}} = 1$ when the Ω_{GW} always stay below the PLISCs (for the details of the PLISCs, see Appendix A of [52]). For example, the GW spectrum for the case with $(\chi_{\text{ini}}, V_0^{1/4}) = (6M_{\text{Pl}}, 10^6 \text{ GeV})$ (red line in the left panel of Fig. 6) gives $q_{\text{DECIGO}} = 229$, $q_{\text{LISA}} = 0.172$.

In Fig. 7, we depict the parameter region where the GW spectrum can be detected in LISA (magenta region) and DECIGO (blue region), i.e., the spectrum can exceed the PLISC for LISA and DECIGO, in the $\chi_{\text{ini}}-V_0$ plane for the power-law potential with $p = 6$ and 8 (top panels), and the axion-type potential with $n = 3$ and 4 (bottom panels). In the figure, we also show the parameter space where $T_2 < T_{\text{BBN}} \sim 1 \text{ MeV}$, in which the success of BBN would be spoiled since the Universe experiences a quasi-de Sitter phase during/after BBN in such a case. Although, in Fig. 7 where the tensor-to-scalar ratio is set to be $r = 10^{-3}$, there exists the parameter space where the GW spectrum can be detected for both LISA and DECIGO, such a region disappears when we take a smaller value of r . We checked

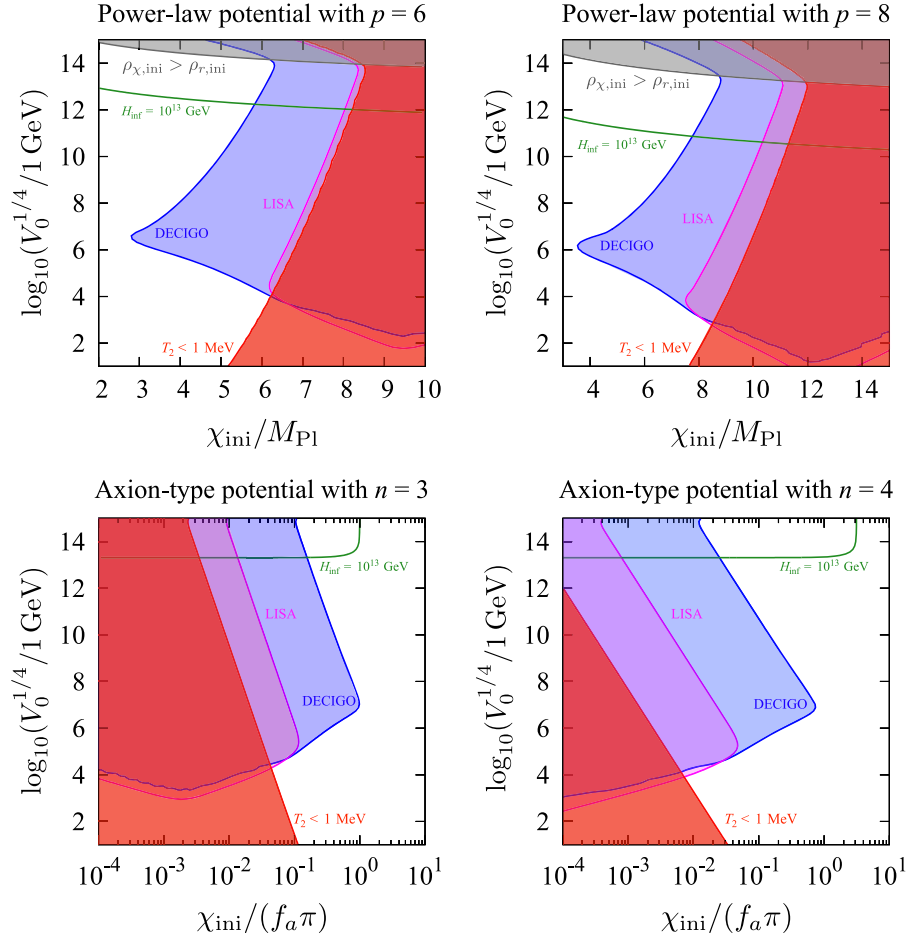


FIG. 7. Detectable region in the $\chi_{\text{ini}}-V_0$ plane. The above panels show the case of the power-law potential with $p = 6$ (top left) and $p = 8$ (top right), while the bottom ones show the case of the axion-type potential with $n = 3$ (bottom left) and $n = 4$ (bottom right). The magenta and blue regions correspond to the parameter space where GWs can be detected in LISA and DECIGO, i.e., $q_{\text{LISA}} \geq 1$ and $q_{\text{DECIGO}} \geq 1$, respectively. The red region corresponds to $T_2 < 1$ MeV, which are prohibited by BBN. The gray region does not satisfy our assumption that the generalized EDE field is subdominant at the time of reheating. The green line shows the prediction of V_0 and χ_{ini} by the stochastic argument in Sec. II C.

that, when $r = 10^{-4}$ ($r = 10^{-5}$), the region with $q_{\text{LISA}} \geq 1$ lies inside the region of $T_2 < T_{\text{BBN}}$ for $p = 6$ ($p = 8$), and hence the detectable region for LISA does not show up. We expect that the SNR for both observations would not exceed q_{thr} as the tensor-to-scalar ratio r gets smaller, but we do not consider such cases.

Furthermore, we only consider the case where the generalized EDE field is subdominant at the time of reheating, i.e., $\rho_\chi(a_R) < \rho_r(a_R)$. In the figure, the gray region corresponds to the one where this condition is not satisfied. Since a larger p (n) gives a steeper increase in the GW spectrum, the case of $p = 8$ ($n = 4$) shows more parameter space for the detection of GWs in the power-law (axion-type) potential.

We also show the predicted values of χ_{ini} and V_0 from the argument of the stochastic approach given in Sec. II C for $H_{\text{inf}} = 10^{13}$ GeV. From the figure, we can see that when the equilibrium distribution for χ field is reached during

inflation, a large (small) value of χ_{ini} can give detectable GWs for the power-law (axion-type) potential with an appropriate choice of V_0 .

C. Implications for recent NANOGrav results

Recently the North American Nanohertz Observatory for Gravitational Waves (NANOGrav) reported evidence of the stochastic GW background from observations of the pulsar timing for 15 years [31], whose signal corresponds to $\Omega_{\text{GW}}^{\text{(NANOGrav)}} \approx 2.5 \times 10^{-8}$ at $f \approx 3.2 \times 10^{-8}$ Hz. If the signal is generated from an inflationary stochastic GW background, one can interpret it with the primordial tensor power spectrum to be extremely blue-tilted, namely $n_T \approx 1.8 \pm 0.3$ [58]. Actually such a blue-tilted spectrum requires a low reheating temperature T_R in order not to violate the BBN constraint [59], and $T_R < 10$ GeV is demanded [58] from the recent NANOGrav signal. Indeed the existence of

the generalized EDE can loosen the limit on T_R and slightly lower n_T to explain the NANOGrav signal. Here we briefly investigate to the implications of the generalized EDE for a blue-tilted spectrum provided that the inflationary GWs explain the NANOGrav signal.

In Fig. 8, we show the GW spectra for the cases with and without the generalized EDE, both of which are assumed to have a blue-tilted tensor spectral index. In every case, the value of n_T is taken such that the scale dependence of the GW spectrum at around NANOGrav frequency is $\Omega_{\text{GW}} \propto f^2$ [31,58]. We also assume the tensor-to-scalar ratio to be $r \simeq 5 \times 10^{-11}$ as in [58], and consider the power-law potential with $p = 6$ (red) and $p = 8$ (blue). Here we take the parameters as $(V_0^{1/4}, \chi_{\text{ini}}, n_T) = (10^{-0.7} \text{ GeV}, 4.3M_{\text{Pl}}, 1.69)$ for $p = 6$ and $(10^{-1.25} \text{ GeV}, 6.2M_{\text{Pl}}, 1.62)$ for $p = 8$, respectively. These parameter sets satisfy the requirement that $T_2 > T_{\text{BBN}} \simeq 1 \text{ MeV}$ to avoid the quasi-de Sitter phase after BBN. We also depict the GW spectrum for the case corresponding to $p \rightarrow \infty$ in which the scaling of the energy density during its oscillating phase is the same as that for the kination-dominated case. For the sake of numerical calculation, we include the case with $p \rightarrow \infty$ by adding an energy component which behaves as

$$\rho_{\text{kin}}(a) = \begin{cases} C_{\text{kin}} & (a \leq a_c), \\ C_{\text{kin}} \left(\frac{a_c}{a}\right)^6 & (a > a_c), \end{cases} \quad (3.7)$$

where C_{kin} is a constant and a_c is the scale factor at which the kination phase starts. Here we take $C_{\text{kin}} = 10^{1.6} \text{ GeV}^4$, $a_c = 10^{-12}$, and $n_T = 1.59$. For the argument involving the kination epoch to explain the NANOGrav results in different frameworks, see e.g., [60,61].

It should be noticed that, with the existence of generalized EDE, the GW spectrum can be enhanced to on top of the blue-tilted primordial GWs. The GW spectrum without the EDE, which is depicted by the dashed magenta line in Fig. 8, assumes $n_T \simeq 1.82$. On the other hand, in the generalized EDE model, the value of n_T can be slightly lowered as shown in Fig. 8. Moreover, the bound on the reheating temperature is relaxed as $T_R < 150 \text{ GeV}$, 400 GeV , and $5 \times 10^3 \text{ GeV}$ for the cases with $p = 6, 8$, and ∞ , respectively. This comes from the fact that the GW amplitude of the modes which enter the horizon during the quasi-de Sitter phase is abruptly suppressed, as shown in Fig. 6. This is a unique feature of the generalized EDE scenario and does not occur in models with a simple kination phase.

IV. CONCLUSION

We have studied the consequences of a scalar field whose energy density can give a non-negligible contribution at some point during the course of the history of the Universe. Such kind of scalar field has recently been discussed as a potential solution to the Hubble tension and is called EDE. In such a EDE model, its energy density gives some contribution at around recombination, and then it quickly dilutes to become a negligible component in later time to be consistent with cosmological observations such as CMB. To realize this situation, the parameters in the scalar-field potential need to be fine-tuned. However, on general grounds, one can take a broad parameter range unless such a parameter choice is motivated by some arguments, and furthermore other cosmological aspects can be affected. We dubbed such an EDE field which can take broad parameter range as ‘‘generalized EDE.’’

In this paper, two different types of potentials for the scalar field χ have been considered: power-law and axion-type ones, in which there are three free parameters; the power index p (or n), the energy scale V_0 , and the initial value χ_{ini} of the scalar field. We have assumed that the energy density of the scalar field is less than that of radiation at the time of reheating.

First, we have investigated to what extent and when the energy density of the generalized EDE field can be sizable as a function of χ_{ini} and V_0 , which was shown in Fig. 4. As discussed in Sec. II, the EDE field can give a non-negligible contribution to the total energy density in a broad

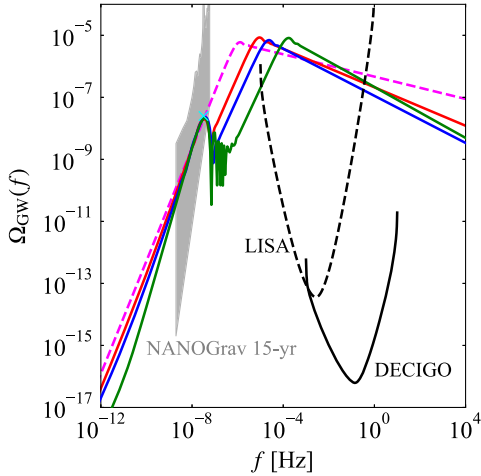


FIG. 8. GW spectra for the power-law potential EDE with $p = 6$ (red line), $p = 8$ (blue line) and $p = \infty$ (green line) for $r = 5.4 \times 10^{-11}$. The values of V_0, χ_{ini} and n_T are assumed such that the spectra can explain the recent NANOGrav signal: $(V_0^{1/4}, \chi_{\text{ini}}, n_T) = (10^{-0.7} \text{ GeV}, 4.3M_{\text{Pl}}, 1.69)$ for $p = 6$ and $(10^{-1.25} \text{ GeV}, 6.2M_{\text{Pl}}, 1.62)$ for $p = 8$. For the case of $p = \infty$, we include such a generalized EDE as a fluid described in the text for the sake of numerical calculation. For comparison, the case without EDE with $n_T = 1.82$ (magenta dashed) is also shown. The gray region corresponds to the recent NANOGrav 15-year signal [32]. The cyan point represents the best-fit value at $f = 1 \text{ yr}^{-1}$ reported by [31]. The black solid and dashed lines represent the PLISCs for DECIGO and LISA, respectively.

parameter range, particularly when $\chi_{\text{ini}} > \mathcal{O}(0.1)M_{\text{pl}} [\chi_{\text{ini}} < \mathcal{O}(0.1)\pi f_a]$ for the power-law (axion-type) potential. Then we studied what values of χ_{ini} and V_0 are suggested from the argument of the stochastic formalism given the inflationary energy scale H_{inf} . In order that the EDE can act as a possible solution to the Hubble tension, one needs $f_{\text{EDE,c}} = \mathcal{O}(0.01)$ and $a_c = \mathcal{O}(10^{-4})$, which can be realized when $\chi_{\text{ini}} = \mathcal{O}(0.1)M_{\text{Pl}}$ and $V_0^{1/4} \sim 10^{-9}$ GeV for the power-law potential and $\chi_{\text{ini}}/f_a \sim 0.9\pi$ and $V_0^{1/4} \sim 10^{-8}$ GeV for the axion-type potential. To realize these values, from Fig. 5, one can see that a low inflationary scale as $H_{\text{inf}} = \mathcal{O}(10^{-9})$ GeV is suggested from the stochastic formalism argument.

We have also investigated the spectrum of the GW background with the existence of the generalized EDE. We have shown that the GW spectrum is amplified as seen in Fig. 6 if the EDE becomes dominant at some epoch, i.e., $f_{\text{EDE}} > 0.5$. The enhancement of the spectrum almost depends on the initial value χ_{ini} which controls the duration of the quasi-de Sitter phase. We studied the parameter ranges for χ_{ini} and V_0 where the GW can be detected by future observations such as LISA and DECIGO, which is shown in Fig. 7.

Finally, we have briefly discussed the implications of the generalized EDE for the NANOGrav 15-year signal, which indicates that $\Omega_{\text{GW}}^{(\text{NANOGrav})} \approx 2.5 \times 10^{-8}$ at $f \approx 3.2 \times 10^{-8}$ Hz.

Assuming that the inflationary GWs can explain the signal, one needs a very blue-tilted primordial tensor power spectrum. In the standard case (i.e., without the generalized EDE), the tensor spectral index n_T should be as large as $n_T \simeq 1.8$ for $r \simeq 5 \times 10^{-11}$ to be well fitted to the signal as in [58]. It should also be noted that, with such a blue-tilted spectrum, the reheating temperature needs to be lowered not to contradict with the BBN constraint and $T_R < 10$ GeV is required [58]. However, with the existence of the EDE and appropriate parameter choices, we found that n_T can be reduced to $n_T = 1.69$ for $p = 6$, $n_T = 1.62$ for $p = 8$, and $n_T = 1.59$ for $p = \infty$. Besides, we also found that the EDE can relax the bound on the reheating temperature to $T_R = 150$ GeV for $p = 6$, $T_R = 400$ GeV for $p = 8$, and $T_R = 1.59$ for $p = \infty$, which can be compared to the case of the standard thermal history $T_R < 10$ GeV [58].

Scalar fields are predicted to ubiquitously exist in the early Universe in the light of high energy theories. The results of this work would help to consider the effects of such a scalar field on the evolution of the Universe.

ACKNOWLEDGMENTS

This work was supported by JSPS KAKENHI Grants No. 19K03874 (T. T.) and No. 23K17691 (T. T.) and MEXT KAKENHI 23H04515 (T. T.).

-
- [1] K. Enqvist and M. S. Sloth, Adiabatic CMB perturbations in pre—big bang string cosmology, *Nucl. Phys.* **B626**, 395 (2002).
 - [2] D. H. Lyth and D. Wands, Generating the curvature perturbation without an inflaton, *Phys. Lett. B* **524**, 5 (2002).
 - [3] T. Moroi and T. Takahashi, Effects of cosmological moduli fields on cosmic microwave background, *Phys. Lett. B* **522**, 215 (2001); **539**, 303(E) (2002).
 - [4] G. Dvali, A. Gruzinov, and M. Zaldarriaga, A new mechanism for generating density perturbations from inflation, *Phys. Rev. D* **69**, 023505 (2004).
 - [5] L. Kofman, Probing string theory with modulated cosmological fluctuations, [arXiv:astro-ph/0303614](https://arxiv.org/abs/astro-ph/0303614).
 - [6] A. Banerjee, H. Cai, L. Heisenberg, E. O. Colgáin, M. M. Sheikh-Jabbari, and T. Yang, Hubble sinks in the low-redshift swampland, *Phys. Rev. D* **103**, L081305 (2021).
 - [7] G. D. Coughlan, W. Fischler, E. W. Kolb, S. Raby, and G. G. Ross, Cosmological problems for the Polonyi potential, *Phys. Lett.* **131B**, 59 (1983).
 - [8] T. Moroi, M. Yamaguchi, and T. Yanagida, On the solution to the Polonyi problem with 0 (10-TeV) gravitino mass in supergravity, *Phys. Lett. B* **342**, 105 (1995).
 - [9] M. Kawasaki, T. Moroi, and T. Yanagida, Constraint on the reheating temperature from the decay of the Polonyi field, *Phys. Lett. B* **370**, 52 (1996).
 - [10] T. Moroi and L. Randall, Wino cold dark matter from anomaly mediated SUSY breaking, *Nucl. Phys.* **B570**, 455 (2000).
 - [11] M. Kamionkowski and A. G. Riess, The Hubble tension and early dark energy, *Annu. Rev. Nucl. Part. Sci.* **73**, 153 (2023).
 - [12] V. Poulin, T. L. Smith, and T. Karwal, The ups and downs of early dark energy solutions to the Hubble tension: A review of models, hints and constraints circa 2023, *Phys. Dark Universe* **42**, 101348 (2023).
 - [13] S. Vagnozzi, Consistency tests of Λ CDM from the early integrated Sachs-Wolfe effect: Implications for early-time new physics and the Hubble tension, *Phys. Rev. D* **104**, 063524 (2021).
 - [14] E. Di Valentino, O. Mena, S. Pan, L. Visinelli, W. Yang, A. Melchiorri, D. F. Mota, A. G. Riess, and J. Silk, In the realm of the Hubble tension—a review of solutions, *Classical Quantum Gravity* **38**, 153001 (2021).
 - [15] L. Perivolaropoulos and F. Skara, Challenges for Λ CDM: An update, *New Astron. Rev.* **95**, 101659 (2022).
 - [16] A. Matsumoto *et al.*, EMPRESS. VIII. A new determination of primordial He abundance with extremely metal-poor galaxies: A suggestion of the lepton asymmetry and implications for the Hubble tension, *Astrophys. J.* **941**, 167 (2022).

- [17] T. Takahashi and S. Yamashita, Big bang nucleosynthesis and early dark energy in light of the EMPRESS Yp results and the H_0 tension, *Phys. Rev. D* **107**, 103520 (2023).
- [18] J. D. Barrow and J. Magueijo, Cosmological constraints on a dynamical electron mass, *Phys. Rev. D* **72**, 043521 (2005).
- [19] T. Sekiguchi and T. Takahashi, Early recombination as a solution to the H_0 tension, *Phys. Rev. D* **103**, 083507 (2021).
- [20] K. Enqvist and S. Nurmi, Non-Gaussianity in curvaton models with nearly quadratic potential, *J. Cosmol. Astropart. Phys.* **10** (2005) 013.
- [21] K. Enqvist and T. Takahashi, Signatures of non-Gaussianity in the curvaton model, *J. Cosmol. Astropart. Phys.* **09** (2008) 012.
- [22] Q.-G. Huang, Curvaton with polynomial potential, *J. Cosmol. Astropart. Phys.* **11** (2008) 005.
- [23] K. Enqvist, S. Nurmi, G. Rigopoulos, O. Taanila, and T. Takahashi, The subdominant curvaton, *J. Cosmol. Astropart. Phys.* **11** (2009) 003.
- [24] K. Enqvist and T. Takahashi, Effect of background evolution on the curvaton non-Gaussianity, *J. Cosmol. Astropart. Phys.* **12** (2009) 001.
- [25] K. Enqvist, S. Nurmi, O. Taanila, and T. Takahashi, Non-Gaussian fingerprints of self-interacting curvaton, *J. Cosmol. Astropart. Phys.* **04** (2010) 009.
- [26] C. T. Byrnes, K. Enqvist, and T. Takahashi, Scale-dependence of non-Gaussianity in the curvaton model, *J. Cosmol. Astropart. Phys.* **09** (2010) 026.
- [27] J. Fonseca and D. Wands, Non-Gaussianity and gravitational waves from quadratic and self-interacting curvaton, *Phys. Rev. D* **83**, 064025 (2011).
- [28] C. T. Byrnes, K. Enqvist, S. Nurmi, and T. Takahashi, Strongly scale-dependent polyspectra from curvaton self-interactions, *J. Cosmol. Astropart. Phys.* **11** (2011) 011.
- [29] T. Kobayashi and T. Takahashi, Runnings in the curvaton, *J. Cosmol. Astropart. Phys.* **06** (2012) 004.
- [30] R. K. Sharma, S. Das, and V. Poulin, Early dark energy beyond slow-roll: Implications for cosmic tensions, *arXiv:2309.00401*.
- [31] G. Agazie *et al.* (NANOGrav Collaboration), The NANOGrav 15 yr data set: Evidence for a gravitational-wave background, *Astrophys. J. Lett.* **951**, L8 (2023).
- [32] A. Afzal *et al.* (NANOGrav Collaboration), The NANOGrav 15 yr data set: Search for signals from new physics, *Astrophys. J. Lett.* **951**, L11 (2023).
- [33] N. Aghanim *et al.* (Planck Collaboration), Planck 2018 results. VI. Cosmological parameters, *Astron. Astrophys.* **641**, A6 (2020); **652**, C4(E) (2021).
- [34] Y. Shtanov, J. H. Traschen, and R. H. Brandenberger, Universe reheating after inflation, *Phys. Rev. D* **51**, 5438 (1995).
- [35] N. Kaloper, Dark energy, H_0 and weak gravity conjecture, *Int. J. Mod. Phys. D* **28**, 1944017 (2019).
- [36] T. Rudelius, Constraints on early dark energy from the axion weak gravity conjecture, *J. Cosmol. Astropart. Phys.* **01** (2023) 014.
- [37] J. Martin and R. H. Brandenberger, The TransPlanckian problem of inflationary cosmology, *Phys. Rev. D* **63**, 123501 (2001).
- [38] R. H. Brandenberger and J. Martin, The robustness of inflation to changes in superPlanck scale physics, *Mod. Phys. Lett. A* **16**, 999 (2001).
- [39] A. Bedroya and C. Vafa, Trans-Planckian censorship and the swampland, *J. High Energy Phys.* **09** (2020) 123.
- [40] D. H. Lyth and A. R. Liddle, *The Primordial Density Perturbation: Cosmology, Inflation and the Origin of Structure* (Cambridge University Press, 2009).
- [41] A. A. Starobinsky and J. Yokoyama, Equilibrium state of a selfinteracting scalar field in the de Sitter background, *Phys. Rev. D* **50**, 6357 (1994).
- [42] A. A. Starobinsky, Stochastic de Sitter (inflationary) stage in the early universe, *Lect. Notes Phys.* **246**, 107 (1986).
- [43] K. Enqvist, R. N. Lerner, O. Taanila, and A. Tranberg, Spectator field dynamics in de Sitter and curvaton initial conditions, *J. Cosmol. Astropart. Phys.* **10** (2012) 052.
- [44] R. J. Hardwick, V. Vennin, C. T. Byrnes, J. Torrado, and D. Wands, The stochastic spectator, *J. Cosmol. Astropart. Phys.* **10** (2017) 018.
- [45] N. Kitajima and T. Takahashi, Stochastic gravitational wave background from early dark energy, *J. Cosmol. Astropart. Phys.* **10** (2023) 074.
- [46] P. A. R. Ade *et al.* (BICEP/Keck Collaboration), Improved constraints on primordial gravitational waves using Planck, WMAP, and BICEP/Keck observations through the 2018 observing season, *Phys. Rev. Lett.* **127**, 151301 (2021).
- [47] S. Kuroyanagi, T. Chiba, and N. Sugiyama, Precision calculations of the gravitational wave background spectrum from inflation, *Phys. Rev. D* **79**, 103501 (2009).
- [48] K. Nakayama, S. Saito, Y. Suwa, and J. Yokoyama, Probing reheating temperature of the universe with gravitational wave background, *J. Cosmol. Astropart. Phys.* **06** (2008) 020.
- [49] K. Nakayama and J. Yokoyama, Gravitational wave background and non-Gaussianity as a probe of the curvaton scenario, *J. Cosmol. Astropart. Phys.* **01** (2010) 010.
- [50] S. Kuroyanagi, T. Takahashi, and S. Yokoyama, Blue-tilted tensor spectrum and thermal history of the universe, *J. Cosmol. Astropart. Phys.* **02** (2015) 003.
- [51] G. Ye and A. Silvestri, Can the gravitational wave background feel wiggles in spacetime?, *Astrophys. J. Lett.* **963**, L15 (2024).
- [52] K. Schmitz, New sensitivity curves for gravitational-wave signals from cosmological phase transitions, *J. High Energy Phys.* **01** (2021) 097.
- [53] A. Klein *et al.*, Science with the space-based interferometer eLISA: Supermassive black hole binaries, *Phys. Rev. D* **93**, 024003 (2016).
- [54] K. Yagi and N. Seto, Detector configuration of DECIGO/BBO and identification of cosmological neutron-star binaries, *Phys. Rev. D* **83**, 044011 (2011); **95**, 109901(E) (2017).
- [55] R. T. Co, D. Dunskey, N. Fernandez, A. Ghalsasi, L. J. Hall, K. Harigaya, and J. Shelton, Gravitational wave and CMB probes of axion kination, *J. High Energy Phys.* **09** (2022) 116.
- [56] Y. Gouttenoire, G. Servant, and P. Simakachorn, Kination cosmology from scalar fields and gravitational-wave signatures, *arXiv:2111.01150*.
- [57] M. Breitbach, J. Kopp, E. Madge, T. Opferkuch, and P. Schwaller, Dark, cold, and noisy: Constraining secluded

- hidden sectors with gravitational waves, *J. Cosmol. Astropart. Phys.* **07** (2019) 007.
- [58] S. Vagnozzi, Inflationary interpretation of the stochastic gravitational wave background signal detected by pulsar timing array experiments, *J. High Energy Astrophys.* **39**, 81 (2023).
- [59] S. Kuroyanagi, T. Takahashi, and S. Yokoyama, Blue-tilted inflationary tensor spectrum and reheating in the light of NANOGrav results, *J. Cosmol. Astropart. Phys.* **01** (2021) 071.
- [60] D. Chowdhury, G. Tasinato, and I. Zavala, Dark energy, D-branes, and pulsar timing arrays, *J. Cosmol. Astropart. Phys.* **11** (2023) 090.
- [61] K. Harigaya, K. Inomata, and T. Terada, Induced gravitational waves with kination era for recent pulsar timing array signals, *Phys. Rev. D* **108**, 123538 (2023).